A Method of Moments Approach for the Efficient and Accurate Modeling of Moderately Thick Cylindrical Wire Antennas

Douglas H. Werner, *Senior Member, IEEE*

***Abstract*— This paper introduces a moment-method formulation, which is capable of accurately modeling moderately thick cylindrical wire antennas. New algorithms are presented for the efficient computation of the cylindrical wire kernel and related impedance matrix integrals. These algorithms make use of exact series representations as well as efficient numerical procedures and lead to a significant reduction in overall computation time for thicker wires. Another major advantage of this moment-method technique is that it is no longer restricted by the segment length-to-radius ratio limitations inherent in past formulations, thereby making it possible to achieve solution convergence for a much wider class of wire antenna structures. Several examples illustrating the superior convergence properties of this new moment-method formulation are presented and discussed.**

***Index Terms*—Cylindrical antennas, moment methods.**

I. Introduction

SEVERAL techniques have been developed over the years for the numerical solution of antenna integral equations of the Hallén as well as Pocklington type. The majority of this work has focused on thin-wire forms of these integral equations, which employ the so-called reduced-kernel approximation [1]–[4]. These techniques are primarily restricted to modeling thin cylindrical wires with radii up to about 0.01λ. Beyond this, the assumptions and approximations upon which these methods are based begin to breakdown, yielding inaccurate results. For this reason, there have been several attempts to generalize these formulations in an effort to extend their range of usefulness.

A survey of cylindrical antenna theory based on early methods for obtaining solutions to Hallén's integral equation for moderately thick tubular wires with narrow gaps is presented in [5]. Two different approaches for solving this form of the cylindrical wire integral equation are considered. The first technique involves iterative solutions that use an approximation to the antenna current as a starting point, while the second consists of converting the integral equation into a set of linear simultaneous equations with Fourier coefficients of the current distribution as unknowns. It was later shown by King and Wu [6] and Chang [7] that the idealized delta-gap generator used in past formulations of Hallén's integral equation were inadequate and would lead to inaccurate results when used to model moderately thick open-ended thin-walled tubular antennas.

An alternative method for numerically evaluating Hallén's integral equation for the moderately thick tubular dipole is presented in [8]. This technique is based on an entire-domain Galerkin procedure, which uses a polynomial representation for the current distribution. The technique was shown to give reasonable results when compared to measurements for dipoles of radii as large as 0.1129λ with lengths down to about 0.4λ. For shorter dipoles, however, significant divergence of the computed curves from experimental results was observed. An integral equation is developed in [9] for the dipole antenna of revolution using the extended boundary condition method originally proposed by Waterman [10]. A subdomain method of moments (MoM) formulation is used to solve the integral equation, which employs a piecewise sinusoidal expansion for the current distribution. The advantage of this procedure is that it leads to an integral equation that is formally exact and has a regular kernel. However, it was found that for moderately thick antennas, numerical instabilities begin to appear as the wire segmentation is increased.

This paper introduces a subdomain MoM approach that has been developed for the accurate and efficient analysis of moderately thick cylindrical wire antennas. Most MoM codes make use of a reduced-kernel approximation to decrease the complexity of the cylindrical wire kernel and its associated expressions. As discussed above, this assumption works well for most wire structures, which have a radius of 0.01λ or less. As the wire radius increases, individual segments in a MoM solution space tend to become very short and thick. Traditionally, a measure of this quantity is referred to as the segment length-to-radius ratio (Δ/a). The majority of thin-wire codes using the reduced-kernel approximation have the restriction that Δ/a should be greater than at least ten at all times to insure accurate results. For most thin-wire problems, this restriction presents no great difficulties. On the other hand, for thicker wires, the model often cannot be sufficiently broken into enough segments and, therefore, convergence in the MoM solution cannot be achieved. However, by retaining the full-kernel expression and reformulating the source model to be more physically representative, it will be demonstrated in this paper that significant reductions in Δ/a are possible. In fact, this technique is capable of maintaining convergence

Manuscript received October 22, 1996; revised September 9, 1997. This work was supported by Lieutenant Commander J. S. Zmyslo of the Naval Information Warfare Activity, Washington, DC.

The author is with the Applied Research Laboratory, The Pennsylvania State University, State College, PA 16804 USA.

Publisher Item Identifier S 0018-926X(98)02259-5.

for so-called "pancake" or "poker-chip" segmentation (i.e., for Δ/a ratios even smaller than 0.05). By essentially removing the restriction on Δ/a, which has plagued cylindrical wire MoM formulations since their inception, it becomes possible to analyze a much wider class of wire antenna structures.

The theoretical foundation for the development of a generalized moderately thick-wire MoM formulation which is independent of the segment length-to-radius ratio Δ/a is introduced in Section II. Also discussed in Section II is a new, more physically realistic, voltage source model developed primarily for use on thicker wires. Section III contains several examples which illustrate the ability of the technique to achieve convergence to measured results for several moderately thick cylindrical wire dipoles, including a quarter wave dipole ($L = 0.25\lambda$) of radius $a = 0.1129\lambda$ which is almost as wide as it is long, i.e., $2a/L = 0.9032$. Finally, techniques for the efficient evaluation of the various moderately thick-wire electric field integrals associated with this MoM formulation are presented and discussed in the Appendix.

II. Theory

The basis functions which will be adopted for use in this paper are of the form [11]

$$I_n(z') = A_n + B_n \sin[\beta(z' - z_n)] + C_n \cos[\beta(z' - z_n)] \quad (1)$$

with z_n the midpoint of the nth segment such that $|z' - z_n| \leq \Delta_n/2$ where Δ_n represents the segment length. This choice of basis functions is commonly used because it represents very well the actual currents, which arise in cylindrical wire applications and, therefore, leads to rapid convergence [12]. These basis functions along with a point matching technique are employed in conjunction with Pocklington's integral equation in such a way that both current and charge satisfy continuity conditions at segment junctions [13]. This approach allows two of the unknown coefficients in (1) to be eliminated, leaving only one constant. Following this procedure leads to a moment-method solution of Pocklington's electric field integral equation for arbitrary wire configurations, which may be expressed as

$$\frac{j\omega\mu}{4\pi}\sum_{n=1}^{N}\int_{-\Delta_n/2}^{\Delta_n/2} I_n(z')G(\rho_m, z_m - z')\,dz' = \hat{s}_m \cdot \overline{E}^i(\rho_m, z_m) \quad (2)$$

where $m = 1, 2, \cdots, N$ and

$$G(\rho_m, z_m - z') = \left[\left\{\hat{s}_m \cdot \hat{z}_m + \frac{1}{\beta^2}\left(\frac{\partial^2}{\partial\rho\partial z}\hat{s}_m \cdot \hat{\rho}_n + \frac{\partial^2}{\partial z^2}\hat{s}_m \cdot \hat{z}_n\right)\right\} \cdot K(z - z')\right]_{\substack{\rho=\rho_m \\ z=z_m}} \quad (3)$$

$$K(z - z') = \frac{1}{2\pi}\int_0^{2\pi} \frac{e^{-j\beta R'}}{R'}\,d\phi' \quad (4)$$

$$R' = \sqrt{(z - z')^2 + \rho^2 + a^2 - 2\rho a\cos\phi'}. \quad (5)$$

The parameters (ρ_m, z_m) represent the midpoint coordinates of the observation segment, $\hat{s}_m$ represents the unit vector in the direction of assumed current on the observation segment, and $\hat{\rho}_n$ and $\hat{z}_n$ are unit vectors for the local coordinate system defined by the source segment. The term $K(z - z')$ defined in (4) is known as the cylindrical wire kernel.

As discussed above, the MoM formulation used here assumes a trigonometric current on each segment of the form defined in (1). This suggests that the electric field due to each of the three components of the current distribution (i.e., uniform, sine, and cosine) must be computed. It can be shown that in order to calculate these fields, it is necessary to evaluate a total of six different expressions (integrals) involving the cylindrical wire kernel. These six expressions are summarized below:

$$\frac{1}{\beta}K(z - z') = \frac{1}{2\pi}\int_0^{2\pi} \frac{e^{-j\beta R'}}{\beta R'}\,d\phi' \quad (6)$$

$$D_z K(z - z') = \frac{1}{\beta^2}\frac{\partial}{\partial z}K(z - z') \quad (7)$$

$$D_\rho K(z - z') = \frac{1}{\beta^2}\frac{\partial}{\partial \rho}K(z - z') \quad (8)$$

$$I(\rho, z; a, \Delta) = \int_{-\Delta/2}^{\Delta/2} K(z - z')\,dz' \quad (9)$$

$$S(\rho, z; a, \Delta) = \frac{1}{\beta}\int_{-\Delta/2}^{\Delta/2} \sin(\beta z')\frac{\partial}{\partial\rho}K(z - z')\,dz' \quad (10)$$

$$C(\rho, z; a, \Delta) = \frac{1}{\beta}\int_{-\Delta/2}^{\Delta/2} \cos(\beta z')\frac{\partial}{\partial\rho}K(z - z')\,dz'. \quad (11)$$

It is possible to further simplify the expressions given in (7) and (8) as well as (10) and (11). Evaluating the derivatives which appear in (7) and (8) leads to the following useful integral representations:

$$D_z K(z - z') = -(z - z')\frac{1}{2\pi}\int_0^{2\pi} \frac{(1 + j\beta R')}{(\beta R')^2}\frac{e^{-j\beta R'}}{R'}\,d\phi' \quad (12)$$

$$D_\rho K(z - z') = -\frac{1}{2\pi}\int_0^{2\pi} (\rho - a\cos\phi')\frac{(1 + j\beta R')}{(\beta R')^2} \cdot \frac{e^{-j\beta R'}}{R'}\,d\phi'. \quad (13)$$

The double integrals of (10) and (11) may be reduced to single integrals of the form

$$S(\rho, z; a, \Delta) = \frac{1}{\pi}\int_0^{\pi} \frac{(\rho - a\cos\phi')}{(\rho^2 + a^2 - 2\rho a\cos\phi')} \times \frac{e^{-j\beta R'}}{\beta R'} \cdot [(z - z')\sin(\beta z') + jR'\cos(\beta z')]\Big|_{z'=-\Delta/2}^{z'=\Delta/2} d\phi' \quad (14)$$

$$C(\rho, z; a, \Delta) = \frac{1}{\pi}\int_0^{\pi} \frac{(\rho - a\cos\phi')}{(\rho^2 + a^2 - 2\rho a\cos\phi')} \times \frac{e^{-j\beta R'}}{\beta R'} \cdot [(z - z')\cos(\beta z') - jR'\sin(\beta z')]\Big|_{z'=-\Delta/2}^{z'=\Delta/2} d\phi' \tag{15}$$

by making use of the fact that

$$\int_{-\Delta/2}^{\Delta/2} \frac{\partial}{\partial\rho}\left\{\frac{e^{-j\beta(R'\pm z')}}{\beta R'}\right\} dz' = \pm(\rho - a\cos\phi')\frac{e^{-j\beta(R'\pm z')}}{\beta R'[R' \pm (z' - z)]}\Bigg|_{z'=-\Delta/2}^{z'=\Delta/2}. \tag{16}$$

The integrals given in (14) and (15) are now in a form where they may be readily integrated numerically. It was found that accurate results may be achieved for the majority of cases by using a very low-order numerical integration scheme, such as a three-point Gaussian quadrature. Finally, it should be pointed out that various useful techniques for evaluating (9) have been discussed elsewhere in the literature [14]–[18] and, therefore, will not be considered here.

For many thin-wire applications sufficient accuracy can be achieved by invoking the reduced-kernel approximation [2]

$$K(z - z') \approx K_0(z - z') = \frac{e^{-j\beta R_0}}{R_0} \tag{17}$$

where

$$R_0 = \sqrt{(z - z')^2 + \rho^2}. \tag{18}$$

This approximation is based on the assumption that the wire radius is vanishingly small, i.e., $a = 0$. The use of this reduced-kernel approximation leads to simplified forms for the expressions, which are given in (6), (9), and (12)–(15). Hence, in the case of the thin-wire reduced-kernel formulation, (6) and (12)–(15) will reduce to simple closed-form expressions, while the double integral of (9) reduces to a single integral given by

$$I_0(\rho, z; a, \Delta) = \int_{-\Delta/2}^{\Delta/2} K_0(z - z')\, dz'. \tag{19}$$

Several techniques have been developed for evaluating this integral, which are summarized in [15] and [18]–[20].

On the other hand, when the full-kernel formulation for thicker wires is used, all six expressions involving the kernel (6), (9), (12)–(15) are nonanalytic. As a consequence of this, the computational overhead for the moderately thick-wire formulation can be significant if an effort is not made to devise efficient algorithms for evaluating these six expressions. Several techniques will be developed in this paper for the efficient as well as accurate analysis of these integrals. This includes treatments based on a recently found exact series representation for the cylindrical wire kernel integral [15], [18] as well as efficient numerical procedures. These techniques will be presented and discussed in detail in Sections A and B of the Appendix.

Either the thin-wire reduced-kernel or the thick-wire full-kernel formulation can be used to calculate the electric fields due to a segment. The effectiveness of these solutions depend on many factors including relative proximity to the source segment and the wire radius under consideration. The reduced-kernel MoM formulation is only valid for relatively thin wires ($a \leq 0.01\lambda$). However, it will be demonstrated in this paper that the upper limit on the validity of this moment-method formulation may be extended by at least a factor of ten to include moderately thick wires with radii in the range $0.01\lambda \leq a \leq 0.1\lambda$. This is accomplished in part by making use of more accurate electric field expressions, which are in terms of the full cylindrical wire kernel (4) rather than the reduced kernel (17).

Many types of source models with varying degrees of complexity have been discussed in the literature [4], [21]–[27]. The most common of these source models is one in which a constant longitudinal electric field is applied over a single segment [4]. This particular model has been extensively used because it is simple and leads to adequate results for most thin-wire applications. However, this approach was found to yield inaccurate results for thicker wires even when a full-kernel formulation is used. This is especially true for cases where the segmentation is chosen such that $\Delta/a \leq 1$. In other words, use of a standard source model where the gap size varies with segmentation will generally not lead to convergence in the method of moments solution for thicker wire antennas.

This problem was eliminated by introducing a new voltage source model in which the essential feature is that the gap size remain fixed. A constant gap source model of this type was first suggested by Tesche [23] for application to the high-frequency moment-method solution of the electric field integral equation. In this paper, a constant gap applied electric field source model is incorporated into the full-kernel MoM formulation outlined above. This results in an efficient as well as accurate moment-method technique, which converges for values of Δ/a sufficiently small for most practical applications, including the modeling of moderately thick wires. Several examples illustrating the superior convergence properties of this new MoM technique are presented and discussed in the following section.

III. Results

A comparison is made in this section between calculated and measured values of input impedance for several moderately thick-wire dipole configurations. The calculations of input impedance were performed using three different MoM formulations. The thin-wire reduced-kernel formulation with a standard variable gap applied E-field voltage source model is one technique that will be considered. The second technique is a thick-wire formulation, which is obtained by replacing the reduced-kernel approximations with their corresponding full-kernel representations given in (6), (9), and (12)–(15). The third and final technique is also a thick-wire formulation, which maintains the same full-kernel treatment of the integrals,

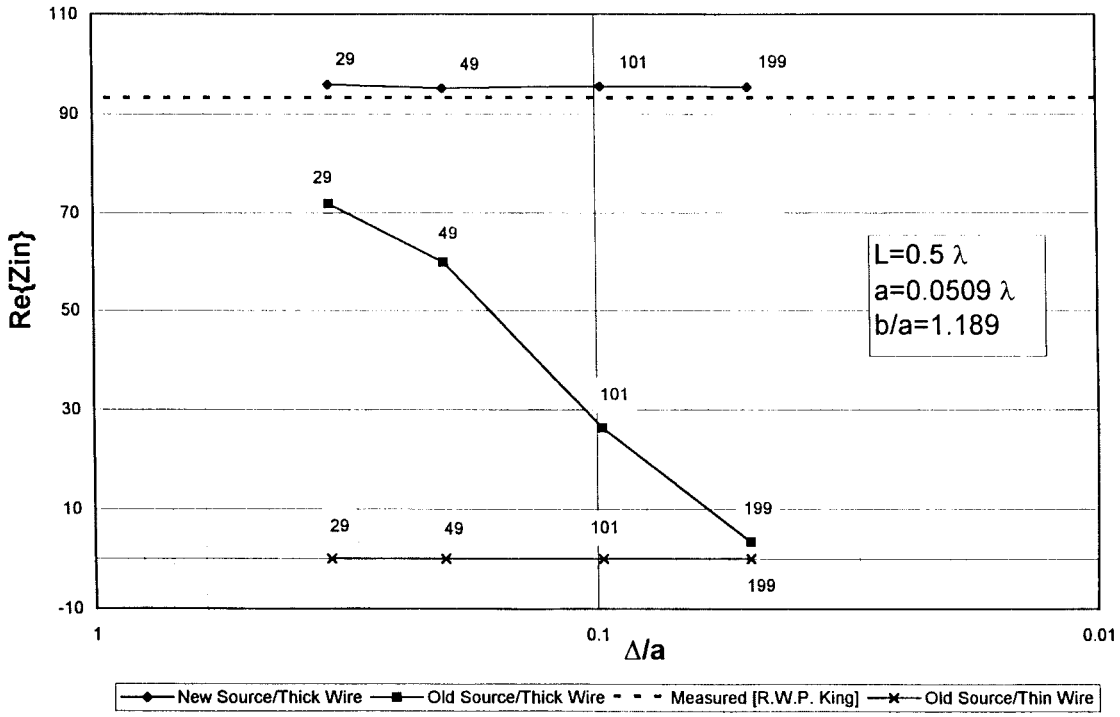

Fig. 1. MoM code predictions for the input resistance in ohms as a function of Δ/a for a half-wave dipole ($L = 0.5\lambda$) of radius $a = 0.0509\lambda$ with a gap width-to-radius ratio $b/a = 1.189$. The measured value of resistance is indicated by the dashed line.

but uses a constant gap rather than a variable gap applied E-field voltage source model. The measured input impedance values were taken from a table of antenna characteristics for moderately thick-wire dipoles compiled by King [28].

Calculated values of input resistance and reactance as a function of wire length-to-radius ratio Δ/a are shown in Figs. 1 and 2, respectively, for a moderately thick half-wave dipole ($L = 0.5\lambda$) with a radius of $a = 0.0509\lambda$ such that $2a/L = 0.2036$. For this example, the gap width of the feed may be expressed in terms of the wire radius as $b = 1.189a$. The measured value of input impedance for this case is indicated by the dashed lines which appear in Fig. 1 (resistance) and Fig. 2 (reactance). The number of segments N corresponding to particular values of Δ/a have been included for reference purposes on the plots. The input impedance values predicted by the variable gap source thin-wire reduced-kernel MoM formulation, referred to as the "old source/thin-wire" formulation, are conveyed in the set of curves marked by the symbol X. As expected, these curves clearly demonstrate the well-known fact that the old source/thin-wire formulation is not valid for application if Δ/a values smaller than about ten are required. In fact, for the small values of Δ/a being considered here, this formulation is predicting an input impedance that is essentially zero. The curves marked by the solid squares represent the input impedance values predicted by the variable gap source thick-wire full-kernel MoM formulation, which we call the "old source/thick-wire" formulation. These curves show that as the segmentation is increased and Δ/a correspondingly decreases, the predicted values of impedance diverge from the measured values. This divergent behavior is linked to the fact that the gap width of the source model is a function of segmentation. In other words, as the wire segment size decreases so does the gap width of the source model. This leads to inaccurate results for thicker wires even though the MoM formulation is based on a full-kernel treatment of the impedance matrix integrals. Finally, the set of curves marked by solid diamonds were generated from the "new source/thick-wire" MoM formulation. The only difference between this formulation and the old source/thick-wire formulation is that the old variable gap-source model has been replaced by a new source model, which maintains a constant gap size independent of segmentation. The plots contained in Figs. 1 and 2 illustrate the superior convergence properties of the new source/thick-wire formulation. Excellent agreement with measurements is maintained for values of Δ/a as small as 0.05.

Now suppose that instead of a moderately thick half-wave dipole of radius 0.0509λ, we consider a quarter-wave dipole ($L = 0.25\lambda$) with a wire radius of $a = 0.1129\lambda$ and a gap width given by $b = 1.189a$. This particular antenna has the property that it is almost as wide as it is long, i.e., $2a/L = 0.9032$. Convergence plots of the input resistance and reactance for this case are shown in Figs. 3 and 4, respectively. Once again, even for this extreme case, the new source/thick-wire formulation consistently yields results which are in excellent agreement with measurements.

The improvement in efficiency gained by employing the thick-wire MoM formulation introduced in this paper may be demonstrated by comparing it to the results obtained when a standard "brute force" numerical approach is used to perform the required full-kernel integrations. For instance, suppose we consider a quarter-wave dipole at 300 MHz ($L = 0.25$ m) with $a = 0.1129$ m and $b = 0.1342$ m. We first use the efficient thick-wire code to calculate the resulting input

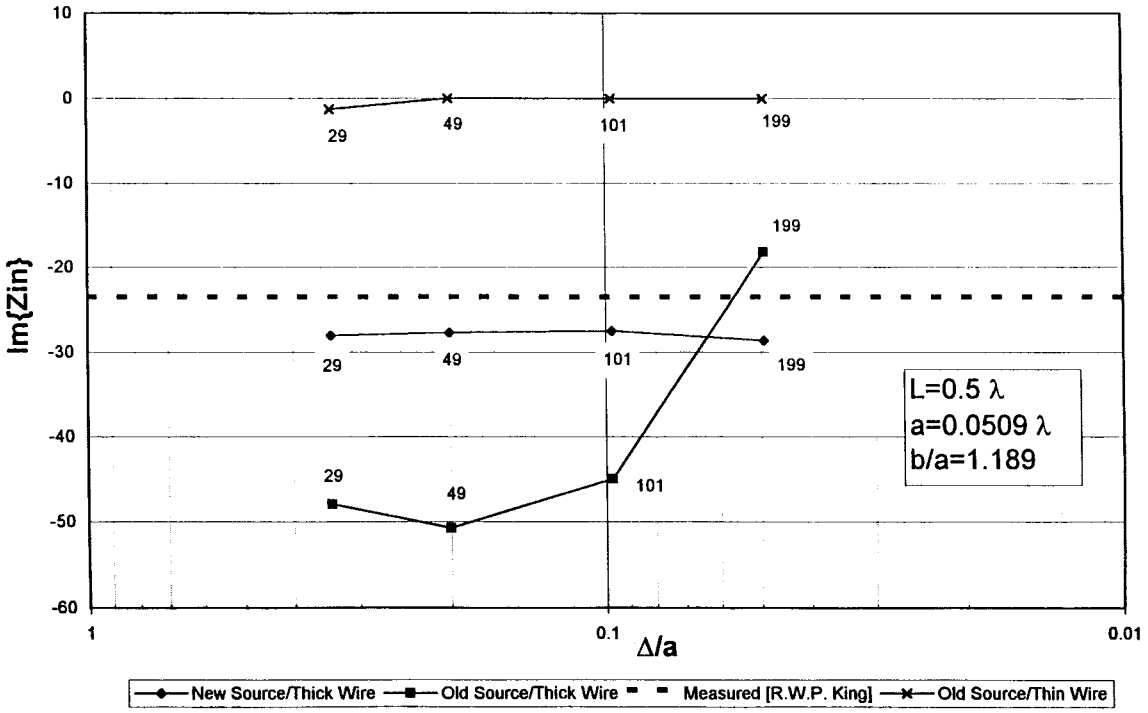

Fig. 2. MoM code predictions for the input reactance in ohms as a function of Δ/a for a half-wave dipole ($L = 0.5\lambda$) of radius $a = 0.0509\lambda$ with a gap width-to-radius ratio $b/a = 1.189$. The measured value of reactance is indicated by the dashed line.

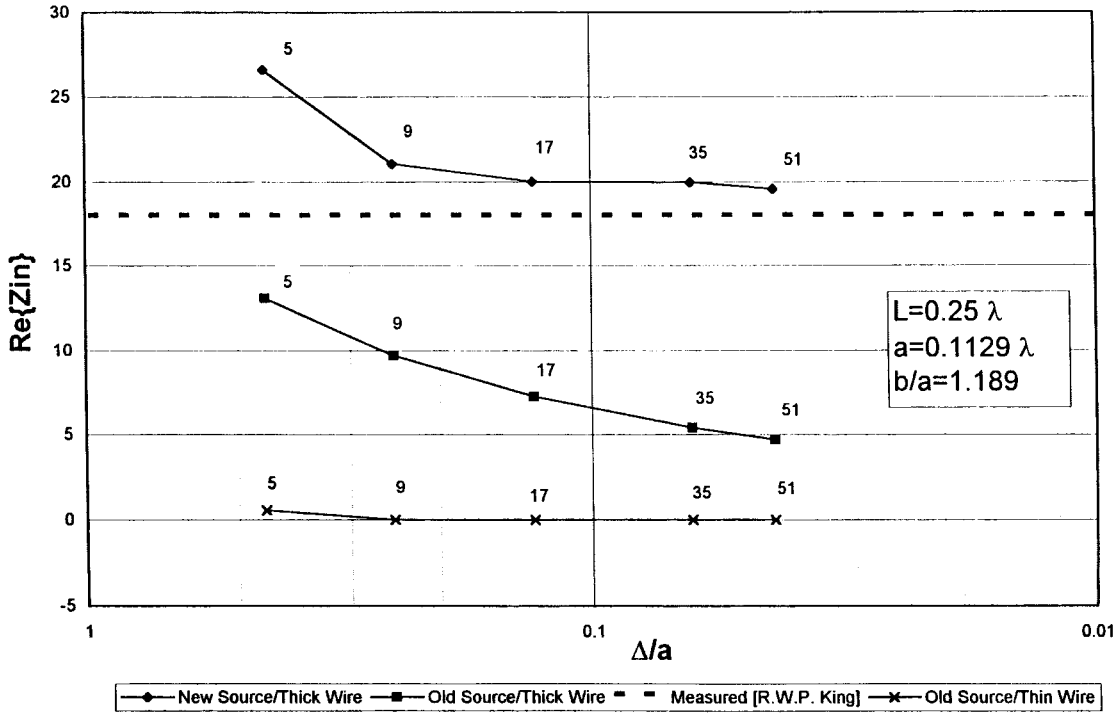

Fig. 3. MoM code predictions for the input resistance in ohms as a function of Δ/a for a quarter-wave dipole ($L = 0.25\lambda$) of radius $a = 0.1129\lambda$ with a gap width-to-radius ratio $b/a = 1.189$. The measured value of resistance is indicated by the dashed line.

impedance which, for a 51-segment model, was found to be $Z_{\text{in}} = 19.528 - j39.569\,\Omega$ (see Figs. 3 and 4). The code was executed on a 120-MHz Pentium computer with a required impedance matrix fill time of 3.46 s. Next, we replace the routines developed for efficient evaluation of the full-kernel integrals with routines which employ a "brute force" numerical integration scheme based on Gaussian quadrature. Table I contains calculated values of input impedance and associated matrix fill times obtained for the same 51-segment quarter-wave dipole example using various orders of Gaussian quadrature integration. These results suggest that comparable accuracy may be achieved by using the efficient thick-wire

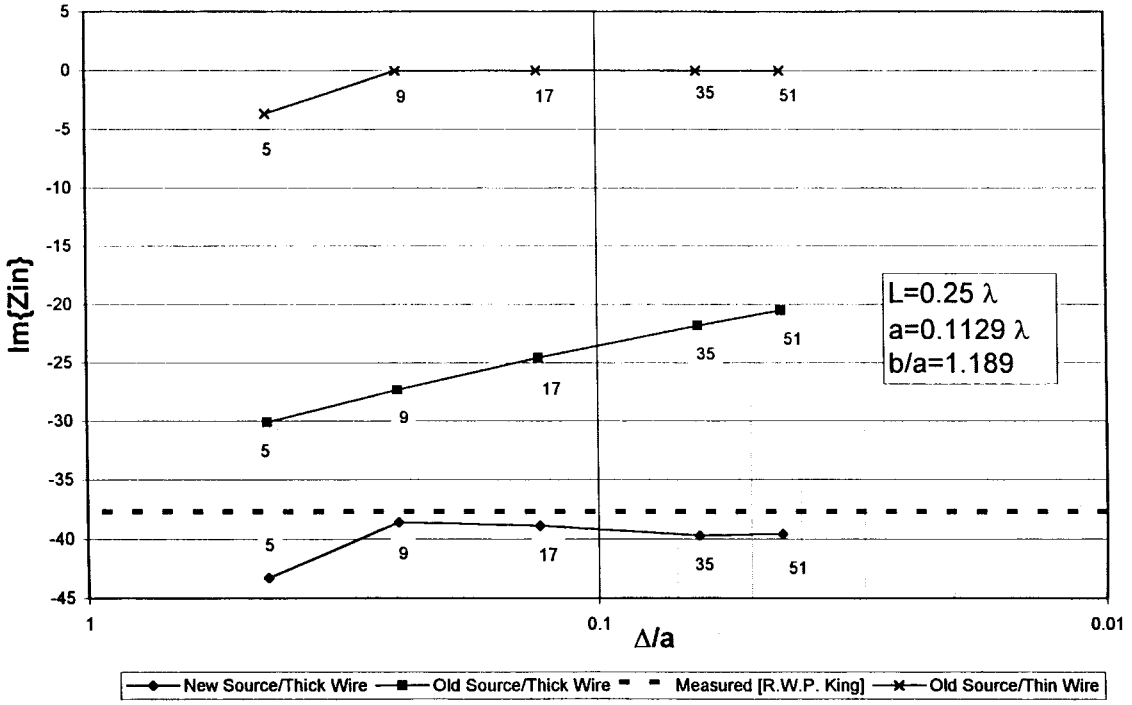

Fig. 4. MoM code predictions for the input reactance in ohms as a function of Δ/a for a quarter-wave dipole ($L = 0.25\lambda$) of radius $a = 0.1129\lambda$ with a gap width-to-radius ratio $b/a = 1.189$. The measured value of reactance is indicated by the dashed line.

TABLE I
INPUT IMPEDANCE AND MATRIX FILL-TIME ESTIMATES FOR A 51-SEGMENT QUARTER-WAVE DIPOLE AT 300 MHz. FULL-KERNEL INTEGRALS ARE EVALUATED NUMERICALLY USING AN N-POINT GAUSSIAN QUADRATURE SCHEME

Gaussian Quadrature (Number of Points)	Z_{in} (Ohms)	Fill Time (Seconds)
6	0.059+j2.009	2.80
8	21.770-j35.761	4.44
10	20.640-j37.124	6.59
12	20.203-j37.974	9.18
14	19.945-j38.508	12.08
16	19.776-j38.869	15.49
18	19.663-j39.121	19.28
20	19.589-j39.293	23.40
22	19.546-j39.406	27.96
24	19.526-j39.476	33.01
26	19.520-j39.517	38.56
28	19.524-j39.537	44.38

formulation with at least a factor of ten reduction in overall computation time.

IV. CONCLUSIONS

Conventional MoM codes, which are based on a reduced-kernel formulation with a variable gap applied E-field voltage source model, are not suitable for application to wires with radii larger than about 0.01λ. A new subdomain MoM formulation was introduced in this paper, which is not only valid for thin wires ($a \leq 0.01\lambda$), but is also valid for moderately thick wires ($0.01\lambda \leq a \leq 0.1\lambda$). This was accomplished by replacing the old thin-wire reduced-kernel treatment with a new thick-wire full-kernel treatment and by reformulating the source model to be more physically representative for thicker wires. It was demonstrated that one of the major advantage of this new MoM technique is that it is no longer restricted by the Δ/a limitations inherent in past formulations and is, therefore, capable of achieving solution convergence for a much wider class of wire antenna structures. Finally, an emphasis has been placed on the development of efficient yet accurate algorithms for the computation of the full kernel and various associated expressions.

APPENDIX

A. Series Representations for $K(z-z')$, $D_z K(z-z')$, and $D_\rho K(z-z')$

Exact series expansions for the cylindrical wire kernel and associated derivatives with respect to z and ρ have recently been derived in [15] and [18]. These expansions provide a means by which the integrals given in (6), (12), and (13) may be efficiently as well as accurately evaluated. A convenient form of these exact series are

$$\frac{1}{\beta}K(z-z') = -\frac{e^{-j\beta R}}{\beta R}\sum_{n=0}^{\infty}\sum_{k=0}^{2n} A_{n,k}\frac{(\beta^2\rho a)^{2n}}{(\beta R)^{2n+k}} \tag{20}$$

$$D_z K(z-z') = \beta(z-z')\frac{e^{-j\beta R}}{(\beta R)^3}\sum_{n=0}^{\infty}\sum_{k=0}^{2n} A_{n,k}\frac{(\beta^2\rho a)^{2n}}{(\beta R)^{2n+k}} \cdot [(2n+k+1)+j\beta R] \tag{21}$$

$$D_\rho K(z-z') = \frac{1}{\beta\rho}\frac{e^{-j\beta R}}{(\beta R)^3}\sum_{n=0}^{\infty}\sum_{k=0}^{2n} A_{n,k}\frac{(\beta^2\rho a)^{2n}}{(\beta R)^{2n+k}} \cdot \{(\beta\rho)^2[(2n+k+1)+j\beta R]-2n(\beta R)^2\} \tag{22}$$

where

$$A_{n,k} = \binom{1/2}{n}\frac{(2n-1)}{(2j)^k}\frac{(2n+k)!}{k!(2n)!(2n-k)!} \tag{23}$$

$$R = \sqrt{(z-z')^2+\rho^2+a^2}. \tag{24}$$

A set of recurrence relations for the efficient computation of the coefficients $A_{n,k}$ (23) have been developed in [15] and [29]. This set of recursions is given by

$$A_{n,0} = \begin{cases} -1, & n=0 \\ -\dfrac{1}{(2n)^2}A_{n-1,0}, & n>0 \end{cases} \tag{25}$$

$$A_{n,k} = \frac{1}{2j}(2n-k+1)\left(\frac{2n+k}{k}\right)A_{n,k-1}. \tag{26}$$

Past methods implemented (20)–(22) using recurrence relations (25) and (26) to increment $A_{n,k}$, while summing over the variable k for each n until some $n_{\max}$ was reached for which the series achieved a specified convergence tolerance. One drawback of these approaches, however, is that they involve calculating terms which are too small to have a significant impact on the series.

A new and more efficient approach for evaluating these series will be presented here that eliminates the need to calculate insignificant terms. We begin the development of this new algorithm by defining a modified expression for (20)

$$\frac{1}{\beta}K(z-z') = -\frac{e^{-j\beta R}}{\beta R}\sum_{n=0}^{\infty}\sum_{k=0}^{2n} F_{n,k} \tag{27}$$

where

$$F_{n,k} = A_{n,k}\frac{(\beta^2\rho a)^{2n}}{(\beta R)^{2n+k}}. \tag{28}$$

This modified form of $A_{n,k}$ leads to the following set of recurrence relations:

$$F_{n,k} = \frac{(-1)(2n+k-1)(2n+k)}{(2n-k-1)(2n-k)(2n)^2}\frac{(\beta^2\rho a)^2}{(\beta R)^2}F_{n-1,k} \tag{29}$$

$$F_{n,k} = \frac{(2n+k-1)(2n+k)}{j(2k)(\beta R)}F_{n,k-1}. \tag{30}$$

Further examination of (30) provides insight into the behavior of the recursion. To find the maximum value of the recursion for a given n, we set $F_{n,k}$ equal to $F_{n,k-1}$ in (30) and solve for k

$$k_{\max} = \tfrac{1}{2}\left[(1-2\beta R)+\sqrt{(1-2\beta R)+8n(2n+1)}\right]. \tag{31}$$

For values of n that are much larger than R, the value at which $F_{n,k}$ reaches a maximum is at $k=2n$. Each value of $F_{n,k}$ for a given n will decrease for decreasing values of k. For this reason, it becomes important to only calculate those values of (20) that are of computational significance. Equation (31) predicts that the maximum recursion value of $F_{n,k}$ for a given n is $F_{n,2n}$, provided that n is sufficiently large. Also, $F_{n,k}$ tends toward smaller values for each succeeding k less than $k=2n$. The recursion in (30) can be run backward from $k=2n$ until the result is smaller than some predefined convergence tolerance. The other noncalculated terms should have little or no impact on the final result and can be ignored.

Before implementing a computationally efficient method for the calculation of (20), it is helpful to define an additional recurrence relation. Combining (29) and (30) yields the following useful relation:

$$F_{n,k} = \frac{(2n+k-3)(2n+k-2)(2n+k-1)(2n+k)}{(2k)(2k-2)(n^2)} \cdot \frac{(\beta^2\rho a)^2}{(\beta R)^3}F_{n-1,k-2} \tag{32}$$

which corresponds to a "diagonal" movement. An efficient implementation of (20) may now be realized by setting a lower limit for k in (27) as follows:

$$\frac{1}{\beta}K(z-z') = -\frac{e^{-j\beta R}}{\beta R}\sum_{n=0}^{\infty}\sum_{k=k_{\min}(n)}^{2n} F_{n,k} \tag{33}$$

where $k_{\min}(n)$ is a lower limit for k based on previous values in the recursion for $F_{n,k}$. Two convergence tolerances are set within the iteration. The first tolerance governs how $k_{\min}(n)$ is incremented as n increases saving a considerable amount of computation. The second convergence tolerance checks that each inner summation in (33) is still large enough to have an impact on the final solution. If not, the summation is assumed to have reached convergence and is therefore terminated.

Previous methods for the computation of (20) summed all values of k for a given value of n. The value of n was incremented until the inner summation term passed below some predefined convergence value. This new method saves much of the computation over the old method by using the $k_{\min}$ value in the inner summation of (33). For most problems of computational interest, $k_{\min}$ remains relatively close to $2n$. For larger values of n, most of the terms calculated in (20) have little or no impact on the final answer. In some cases, over 80% of the terms calculated using previous methods could be ignored using this new method.

Finally, it is now possible to derive a useful convergence property of (33) and, hence, (20). For large values of a and small values of R, the expressions tend to converge slowly or not at all. A quantitative measure of the convergence of these expressions can be calculated by making use of (32). When the maximum value for the recursion (31) is substituted into (32) and simplified for large values of n, the following expression is obtained:

$$F_{n,k} = \frac{4(\rho a)^2}{R^4}F_{n-1,k-2}. \tag{34}$$

Careful examination of (34) and (24) reveals that $F_{n,k}$ in (33) will always tend to approach zero. However, from the computational point of view, the rate of convergence is a very important factor in determining the efficiency of the method.

To apply the same results to the derivatives of the kernel, we start with simplified expressions for the derivatives given by

$$D_z K(z-z') = \beta(z-z')\frac{e^{-j\beta R}}{(\beta R)^3}\sum_{n=0}^{\infty}\sum_{k=0}^{2n} F_{n,k}^1 \tag{35}$$

$$D_\rho K(z-z') = \frac{1}{\beta\rho}\frac{e^{-j\beta R}}{(\beta R)^3}\left[\left(\sum_{n=0}^{\infty}\sum_{k=0}^{2n} F_{n,k}^2\right) - \left(\sum_{n=0}^{\infty}\sum_{k=0}^{2n} F_{n,k}^3\right)\right] \tag{36}$$

where

$$F_{n,k}^1 = F_{n,k}[(2n+k+1) + j\beta R] \tag{37}$$

$$F_{n,k}^2 = F_{n,k}(\beta\rho)^2[(2n+k+1) + j\beta R] \tag{38}$$

$$F_{n,k}^3 = F_{n,k}(2n)(\beta R)^2. \tag{39}$$

From (37)–(39), it is easy to see that all of the derivative terms fall off as fast or faster than $F_{n,k}$ for decreasing values of k. Thus, with slight modification, a routine designed to calculate the kernel can be made to simultaneously compute both the derivative terms with little increase in overall computational time. Also, the lower bound $k_{\min}(n)$ will apply to the calculation of the derivative terms as well.

B. Numerical Methods for Evaluating $K(z-z')$, $D_z K(z-z')$, and $D_\rho K(z-z')$

In Appendix A, series forms of the kernel and the associated derivatives of the kernel were presented. Also, a fast method for the calculation of these expressions was introduced. However, field points that are in close proximity to the source segment of moderately thick wires can cause numerical instability in the calculation of these exact expressions. For these cases, a large number of terms is needed for convergence and other methods become more attractive for the calculation of these expressions. One such method for the calculation of (6), (12), and (13) has been developed in [15], which involves complete elliptic integrals of the first, second, and third kinds.

The cylindrical wire kernel can be split into two integrals—one in which the integrand is singular and the other in which the integrand is slowly varying—that may be treated separately

$$\frac{1}{\beta}K(z-z') = \frac{1}{2\pi}\left[\int_0^{2\pi}\frac{1}{\beta R'}\,d\phi' + \int_0^{2\pi}\frac{e^{-j\beta R'}-1}{\beta R'}\,d\phi'\right]. \tag{40}$$

The second integral in (40) contains an integrand that is slowly varying and can be integrated using a relatively low-order numerical integration scheme such as three-point Gaussian quadrature. The first integral can be expressed in the form [15]

$$\frac{1}{\pi}\int_0^{\pi}\frac{1}{\beta R'}\,d\phi' = \frac{1}{\pi}\frac{1}{\beta\sqrt{\rho a}}kF\left(\frac{\pi}{2},k\right), \quad 0 \le k < 1 \tag{41}$$

where

$$F\left(\frac{\pi}{2},k\right) = \int_0^{\pi/2}\frac{d\varphi}{\sqrt{1-k^2\sin^2\varphi}} \tag{42}$$

represents a complete elliptic integral of the first kind and

$$k = \frac{2\sqrt{\rho a}}{\sqrt{(z-z')^2+(\rho+a)^2}}. \tag{43}$$

Expressions for the derivatives of the kernel may be found by following a similar procedure. Performing the indicated differentiation of the integral form of the kernel yields the following results:

$$D_z K(z-z') = -\beta(z-z')\Im_1(z-z',\rho,a) \tag{44}$$

$$D_\rho K(z-z') = (\beta a)\Im_2(z-z',\rho,a) - (\beta\rho)\Im_1(z-z',\rho,a) \tag{45}$$

where

$$\Im_1(z-z',\rho,a) = \frac{1}{\pi}\int_0^{\pi}[1+j\beta R']\frac{e^{-j\beta R'}}{(\beta R')^3}\,d\phi' \tag{46}$$

$$\Im_2(z-z',\rho,a) = \frac{1}{\pi}\int_0^{\pi}[1+j\beta R']\frac{e^{-j\beta R'}}{(\beta R')^3}\cos\phi'\,d\phi'. \tag{47}$$

The integrals (46) and (47) can be evaluated numerically, but the results will be inadequate for points calculated in the vicinity of the singularity. Extracting the singularity from $\Im_1$ leads to

$$\begin{aligned}\Im_1(z-z',\rho,a) &= \frac{1}{2\pi(\beta^2\rho a)^{1/2}}kF\left(\frac{\pi}{2},k\right) + \frac{1}{4\pi(\beta^2\rho a)^{3/2}}\\ &\quad\cdot\frac{k^3}{1-k^2}E\left(\frac{\pi}{2},k\right) + \frac{1}{\pi}\\ &\quad\cdot\int_0^{\pi}\left\{\frac{[1+j\beta R']e^{-j\beta R'} - [1+(\beta R')^2/2]}{(\beta R')^3}\right\}\\ &\quad\cdot d\phi', \qquad \rho \ne a\end{aligned} \tag{48}$$

where

$$E\left(\frac{\pi}{2},k\right) = \int_0^{\pi/2}\sqrt{1-k^2\sin^2\varphi}\,d\varphi \tag{49}$$

is a complete elliptic integral of the second kind. For the case where $\rho = a$, (48) reduces to

$$\begin{aligned}\Im_1(z-z',a,a) &= \frac{1}{2\pi(\beta a)}kF\left(\frac{\pi}{2},k\right) + \frac{1}{4\pi(\beta a)^3}\\ &\quad\cdot\frac{k^3}{1-k^2}E\left(\frac{\pi}{2},k\right) + \frac{1}{\pi}\\ &\quad\cdot\int_0^{\pi}\left\{\frac{[1+j\beta R']e^{-j\beta R'} - [1+(\beta R')^2/2]}{(\beta R')^3}\right\}d\phi'\\ &\quad z \ne z'.\end{aligned} \tag{50}$$

A similar singularity extraction procedure may be followed in order to arrive at an expression for $\Im_2$ given by

$$\begin{aligned}\Im_2(z-z',\rho,a) &= \frac{1}{2\pi(\beta^2\rho a)^{3/2}}\left[\left\{(\beta^2\rho a)\frac{(2-k^2)}{k}-k\right\}F\left(\frac{\pi}{2},k\right)\right. \\ &\quad + \frac{k(2-k^2)}{2(1-k^2)}E\left(\frac{\pi}{2},k\right)-(\beta^2\rho a)\frac{2(1-k^2)}{k} \\ &\quad \left.\cdot\,\Pi\left(\frac{\pi}{2},k^2,k\right)\right]+\frac{1}{\pi} \\ &\quad \cdot\int_0^{\pi}\left\{\frac{[1+j\beta R']e^{-j\beta R'}-[1+(\beta R')^2/2]}{(\beta R')^3}\right\} \\ &\quad \cdot\cos\phi'\,d\phi', \qquad \rho\neq a \end{aligned} \tag{51}$$

where

$$\Pi\left(\frac{\pi}{2},k^2,k\right)=\int_0^{\pi/2}\frac{d\varphi}{(1-k^2\sin^2\varphi)\sqrt{1-k^2\sin^2\varphi}} \tag{52}$$

is a complete elliptic integral of the third kind. For the case in which $\rho = a$, (51) reduces to

$$\begin{aligned}\Im_2(z-z',a,a) &= \frac{1}{2\pi(\beta a)^3}\left\{\left[(\beta a)^2\frac{(2-k^2)}{k}-k\right]F\left(\frac{\pi}{2},k\right)\right. \\ &\quad \cdot\frac{k(2-k^2)}{2(1-k^2)}E\left(\frac{\pi}{2},k\right)-(\beta a)^2\frac{2(1-k^2)}{k} \\ &\quad \left.\cdot\,\Pi\left(\frac{\pi}{2},k^2,k\right)\right\}+\frac{1}{\pi} \\ &\quad \cdot\int_0^{\pi}\left\{\frac{[1+j\beta R']e^{-j\beta R'}-[1+(\beta R')^2/2]}{(\beta R')^3}\right\} \\ &\quad \cdot\cos\phi'\,d\phi' \qquad z\neq z'. \end{aligned} \tag{53}$$

Given that efficient algorithms exist for the calculation of the elliptic integrals [30] and that the singularities in the expressions for the kernel and associated derivatives have been removed, these expressions can be used anywhere in the MoM problem as a rigorous solution. For most of the expressions in the moment-method impedance matrix, this method is too slow to be of computational value when compared to the fast implementation of the series expressions in Appendix A. However, at the points where the series representations fail to converge quickly or at all, these expressions can be used. In most moment-method problems, the fast series method is used for a majority of the problem, and the singularity free elliptic integral method discussed in this section is used for self (i.e., $\rho = a, z = 0$ and $z' = \pm\Delta/2$) and nearby segments, which constitute only a small portion of the total problem.

Two different methods have been presented for calculating the kernel and the two derivatives of the kernel with respect to ρ and z. A method based on exact series formulations was presented in Appendix A, which was used for nonself and less critical terms. A more numerically rigorous formulation based on the evaluation of generalized elliptic integrals (discussed in this section) is used for more critical cases. If the following condition is satisfied:

$$\frac{\rho a}{\sqrt{(z-z')^2+\rho^2+a^2}} > 0.15 \tag{54}$$

then the more computationally intensive elliptic integral forms must be used. Otherwise, the exact series solutions are employed. This cutoff was derived through numerical investigation using (34) as the starting point.

ACKNOWLEDGMENT

The author would like to thank J. A. Huffman and S. E. Metker for their assistance.

REFERENCES

[1] K. K. Mei, "On the integral equations of thin wire antennas," *IEEE Trans. Antennas Propagat.*, vol. AP-13, pp. 374–378, May 1965.
[2] R. W. P. King, "The linear antenna—Eighty years of progress," *Proc. IEEE*, vol. 55, pp. 2–16, Jan. 1967.
[3] C. M. Butler and D. R. Wilton, "Analysis of various numerical techniques applied to thin-wire scatterers," *IEEE Trans. Antennas Propagat.*, vol. AP-23, pp. 534–540, July 1975.
[4] R. F. Harrington, *Field Computation by Moment Methods*. New York: Macmillan, 1968.
[5] R. H. Duncan and F. A. Hinchey, "Cylindrical antenna theory," *J. Research*, vol. 64D, no. 5, pp. 569–584, Sept./Oct. 1960.
[6] R. W. P. King and T. T. Wu, "The thick tubular transmitting antenna," *Radio Sci.*, vol. 2, no. 9, pp. 1061–1065, Sept. 1967.
[7] D. C. Chang, "On the electrically thick cylindrical antenna," *Radio Sci.*, vol. 2, no. 9, pp. 1043–1060, Sept. 1967.
[8] P. G. Rogers and M. W. Gunn, "An entire-domain Galerkin analysis of the moderately thick dipole," *IEEE Trans. Antennas Propagat.*, vol. AP-28, pp. 117–121, Jan. 1980.
[9] C. D. Taylor and D. R. Wilton, "The extended boundary condition solution of the dipole antenna of revolution," *IEEE Trans. Antennas Propagat.*, vol. AP-20, pp. 772–776, Nov. 1972.
[10] P. C. Waterman, "New formulation of acoustic scattering," *J. Acoust. Soc. Amer.*, vol. 45, pp. 1417–1429, June 1969.
[11] Y. S. Yeh and K. K. Mei, "Theory of conical equiangular-spiral antennas: Part I—Numerical technique," *IEEE Trans. Antennas Propagat.*, vol. AP-15, pp. 634–639, Sept. 1967.
[12] E. K. Miller and F. J. Deadrick, "Some computational aspects of thin-wire modeling," in *Numerical and Asymptotic Techniques in Electromagnetics*, R. Mittra, Ed. New York: Springer-Verlag, 1975, pp. 89–127.
[13] G. J. Burke and A. J. Poggio, "Numerical electromagnetics code (NEC)—Method of moments," Rep. NOSC TD 116, Lawrence Livermore Lab., Livermore, CA, Jan. 1981.
[14] D. H. Werner, J. A. Huffman, and P. L. Werner, "Techniques for evaluating the uniform current vector potential at the isolated singularity of the cylindrical wire kernel," *IEEE Trans. Antennas Propagat.*, vol. 42, pp. 1549–1553, Nov. 1994.
[15] ———, "Analytical and numerical methods for evaluating electromagnetic field integrals associated with current-carrying wire antennas," in *Advanced Electromagnetism: Foundations, Theory, Applications*, T. W. Barrett and D. M. Grimes, Eds. Singapore: World Scientific, 1995, pp. 682–762.
[16] S.-O. Park and C. A. Balanis, "Efficient kernel calculation of cylindrical antennas," *IEEE Trans. Antennas Propagat.*, vol. 43, pp. 1328–1331, Nov. 1995.
[17] D. H. Werner and V. Fotopolous, "An efficient technique for self-term evaluation of the uniform current vector potential integrals," *J. Electromagn. Waves Applicat.*, vol. 10, pp. 1595–1600, 1996.
[18] D. H. Werner, "An exact formulation for the vector potential of a cylindrical antenna with uniformly distributed current and arbitrary radius," *IEEE Trans. Antennas Propagat.*, vol. 41, pp. 1009–1018, Aug. 1993.
[19] D. H. Werner, P. L. Werner, J. A. Huffman, A. J. Ferraro, and J. K. Breakall, "An exact solution of the generalized exponential integral and its application to moment method formulations," *IEEE Trans. Antennas Propagat.*, vol. 41, pp. 1716–1719, Dec. 1993.
[20] D. H. Werner, "Author's reply to the comments of A. E. Gera," *IEEE Trans. Antennas Propagat.*, vol. 42, pp. 1201–1202, Aug. 1994.

[21] E. K. Miller, "Admittance dependence of the infinite cylindrical antenna upon exciting gap thickness," *Radio Sci.*, vol. 2, no. 12, pp. 1431–1435, Dec. 1967.
[22] R. A. Hurd and J. Jacobsen, "Admittance of an infinite cylindrical antenna with realistic gap field," *Electron. Lett.*, vol. 4, no. 19, pp. 420–421, Sept. 1968.
[23] F. M. Tesche, "The effect of the thin-wire approximation and the source gap model on the high-frequency integral equation solution of radiating antennas," *IEEE Trans. Antennas Propagat.*, vol. AP-20, pp. 210–211, Mar. 1972.
[24] T. Do-Nhat and R. H. MacPhie, "The static electric field distribution between two semi-infinite circular cylinders: A model for the feed gap of a dipole antenna," *IEEE Trans. Antennas Propagat.*, vol. AP-35, pp. 1273–1280, Nov. 1987.
[25] D. J. J. van Rensburg and D. A. McNamara, "On quasistatic source models for wire dipole antennas," *Microwave Opt. Technol. Lett.*, vol. 3, no. 11, pp. 396–398, Nov. 1990.
[26] G. P. Junker, A. A. Kishk, and A. W. Glisson, "A novel delta gap source model for center fed cylindrical dipoles," *IEEE Trans. Antennas Propagat.*, vol. 43, pp. 537–540, May 1995.
[27] G. P. Junker, A. W. Glisson, and A. A. Kishk, "On the stability of simple voltage source models for the study of mutual coupling effects," in *12th Annu. Rev. Progress Appl. Comput. Electromagn.*, Monterey, CA, Mar. 1996, pp. 842–847.
[28] R. W. P. King, *Table of Antenna Characteristics.* New York: IFI/Plenum, 1971.
[29] J. A. Huffman, "Numerical modeling of current-carrying wire antennas using exact expressions for the vector potential and electric field integrals," Ph.D. dissertation, Dept. Elect. Eng., The Pennsylvania State Univ., University Park, PA, May 1995.
[30] W. H. Press, S. A. Teukolsky, W. T. Vettering, and B. P. Flannery, *Numerical Recipes in Fortran, The Art of Scientific Computing*, 2nd ed. New York: Cambridge Univ. Press, 1992.

Douglas H. Werner (S'81–M'89–SM'94) received the B.S., M.S., and Ph.D. degrees in electrical engineering from The Pennsylvania State University, University Park, PA, in 1983, 1985, and 1989, respectively, and the M.A. degree in mathematics from the same university in 1986.

He is a Senior Research Associate in the Communications Department of the Applied Research Laboratory, The Pennsylvania State University. He is also a member of the Graduate Faculty in the Pennsylvania State University Department of Electrical Engineering. He has published over 50 technical papers and proceedings articles and is the author of two book chapters. His research interests include theoretical and computational electromagnetics, antenna theory and design, electromagnetic wave interaction with complex materials, fractal and knot electrodynamics, and genetic algorithms.

Dr. Werner was presented with the 1993 Applied Computational Electromagnetics Society (ACES) Best Paper Award and was also the recipient of a 1993 International Union of Radio Science (URSI) Young Scientist Award. In 1994, he received The Pennsylvania State University Applied Research Laboratory Outstanding Publication Award. He has also received several Letters of Commendation from The Pennsylvania State University Department of Electrical Engineering for outstanding teaching and research. He is a member of the American Geophysical Union (AGU), URSI Commissions B and G, the Applied Computational Electromagnetics Society (ACES), Eta Kappa Nu, Tau Beta Pi, and Sigma Xi.